Multimodality Imaging of Pericardial Diseases

Kibar Yared, MD,*‡ Aaron L. Baggish, MD,* Michael H. Picard, MD,*
Udo Hoffmann, MD,† Judy Hung, MD*

Boston, Massachusetts; and Toronto, Ontario, Canada

Pericardial disease is an important cause of morbidity and mortality in patients with cardiovascular disease. Inflammatory diseases of the pericardium constitute a spectrum ranging from acute pericarditis to chronic constrictive pericarditis. Other important entities that involve the pericardium include benign and malignant pericardial masses, pericardial cysts, and diverticula, as well as congenital absence of the pericardium. Recent advances in multimodality noninvasive cardiac imaging have solidified its role in the management of patients with suspected pericardial disease. The physiologic and structural information obtained from transthoracic echocardiography and the anatomic detail provided by cardiac computed tomography and magnetic resonance have led to growing interest in the complementary use of these techniques. Optimal management of the patient with suspected pericardial disease requires familiarity with the key imaging modalities and the ability to choose the appropriate imaging tests for each patient. This report reviews the imaging modalities most useful in the assessment of patients with pericardial disease, with an emphasis on the complementary value of multimodality cardiac imaging. (J Am Coll Cardiol Img 2010;3:650–60) © 2010 by the American College of Cardiology Foundation

Pericardial disease is an important cause of morbidity and mortality in patients with cardiovascular disease. Inflammatory diseases of the pericardium constitute a spectrum ranging from acute pericarditis (AP) to chronic constrictive pericarditis (CP). Pericardial masses, cysts, and diverticula as well as congenital absence of the pericardium comprise the remainder of entities that involve the pericardium.

The accurate diagnosis of pericardial disease is a well-recognized clinical challenge that often requires the integration of medical history, physical examination, imaging, and invasive hemodynamic measurements. Recent advances in multimodality noninvasive cardiac imaging have confirmed its essential role in the diagnosis and management of patients with suspected pericardial disease. There is an ex-tensive body of evidence describing the important role of transthoracic echocardiography (TTE) in diagnosing pericardial pathology and its ability to accurately estimate hemodynamic compromise from pericardial disease. More recently, the detailed anatomic characterization of the pericardium provided by cardiac computed tomography (CCT) and cardiac magnetic resonance (CMR) has aided in determining the etiology of pericardial pathology. Optimal management of the patient with suspected pericardial disease requires familiarity with the key imaging modalities and the ability to choose the appropriate imaging tests for each patient. This report reviews the common imaging modalities in the assessment of patients with pericardial disease, with an emphasis on the complementary value of multimodality cardiac imaging.

Normal Pericardial Anatomy, Physiology, and Appearance on Cardiac Imaging

Pericardial anatomy. The pericardium is an avascular fibrous sac that surrounds the heart. It consists of 2 layers: the inner serosal layer and the outer fibrous pericardium. The inner serosal layer is further comprised of a visceral and parietal pericardium (1,2). A potential space separates the visceral and the parietal serosal layers and normally contains up to 50 ml of serous fluid distributed mostly over the atrioventricular and interventricular grooves.

Appearance on echocardiography. The normal pericardium is a thin, linear structure that is typically not visualized directly by echocardiography but rather is outlined as a bright, highly echogenic line from its interface with lung tissue. However, if there is significant thickening (>5 mm) of either pericardial layer, visualization by echocardiography becomes possible. Normally, pericardial fluid can only be seen in systole. As fluid accumulates within the pericardial space, it becomes visible throughout the cardiac cycle. The heart and visceral pericardium normally slide or twist within, and independently of, the parietal pericardium.

Appearance on CCT. With CCT, the normal pericardium is best imaged in systole and appears as a line of average thickness of 1.3 to 2.5 mm (almost always <4 mm) (3); CCT delineates the pericardium as a bright, linear structure that is easily detectable in both contrast- and noncontrast-enhanced examinations because of its visibility against the low attenuation of the surrounding fat. Visualization of the pericardium varies with location and is sometimes difficult against the lateral, posterior, and inferior left ventricular wall because of a paucity of pericardial fat.

Appearance on CMR. CMR delineates the normal pericardium as a curvilinear line of low signal intensity between the myocardium and pericardial fat both on electrocardiogram-gated T_1-weighted spin echo and gradient echo sequences. Visualization of the visceral pericardium often depends on the amount and extent of epicardial fat. In most cases, the pericardium is best seen along the mid level of the anterior right ventricular surface (Fig. 1) (4). Contrast media administration may be necessary to demarcate the pericardium when there is a lack of epicardial fat. Visualization of the pericardium varies with location, as with CCT.

Echocardiography versus CCT versus CMR. Echocardiography remains the primary and first-line imaging modality for diagnosing pericardial disease. It is widely available, cost effective, can be performed portably and quickly, and does not require radiation and intravenous contrast to outline the pericardial space. Importantly, it also provides critical physiologic data in patients with hemodynamic compromise. Poor echocardiographic windows in certain patients and the lack of anatomic detail of the pericardium often serve as limitations of imaging with this modality.

CCT has a relatively quick acquisition time and provides excellent morphological characterization of the pericardium. It can also help quantify pericardial fat, a marker of cardiovascular disease (5). Unfortunately, contrast administration (limited in those with renal dysfunction) and radiation exposure preclude the more widespread use of this modality. Efforts are currently underway to reduce the total radiation dose of each examination (6). In addition, the discovery of extracardiac lesions has certain advantages and disadvantages (7). CMR provides superior soft tissue and pericardial anatomic characterization, yet it is the most costly of the 3 imaging methods and the acquisition protocol is the most time consuming.

Acute Pericarditis

Acute inflammation of the pericardium, with or without an associated pericardial effusion, can occur as an isolated problem or as a manifestation of systemic disease (8–10).

Echocardiography. TTE is often recommended in patients with suspected AP because it provides a rapid and accurate assessment of the pericardium and underlying cardiac function. In uncomplicated AP, there are usually no abnormal findings. The presence of a pericardial effusion helps to confirm the diagnosis, and a number of echocardiographic criteria have been described to diagnose or exclude the presence of tamponade physiology (discussed below in the Pericardial Tamponade section) (11,12).

CCT. On CCT, pericardial thickening is suggestive of AP. As the duration of pericardial inflammation increases, the once smooth pericardium may develop irregular contours (13). In the case of a pericardial effusion, attenuation measurements enable its initial characterization. Simple serous effusions (transudates) usually have the same attenua-
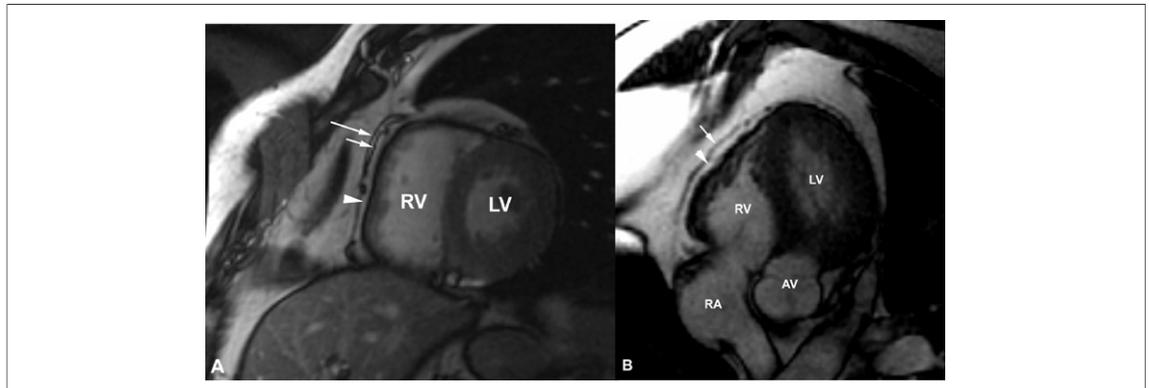
Figure 1. CMR of Normal Pericardium

The CMR bSSFP sequence in short-axis **(left)** and 4-chamber view **(right)** showing the normal pericardial outline and the epicardial fat layer **(arrowhead)**. The **left panel** shows a trivial pericardial effusion separating the visceral **(short arrow)** and parietal **(long arrow)** pericardium. In the **right panel**, the separation is not as evident **(long arrow)** and visualization of the pericardial contour is difficult on the lateral border of the LV. AV = aortic valve; bSSFP = balanced steady-state free precession; CMR = cardiac magnetic resonance; LV = left ventricle; RA = right atrium; RV = right ventricle.

tion as water but vary with cell and protein concentration (0 to 25 HU). Attenuation >25 HU suggests a nonserous fluid composition (exudate) such as those seen in malignancy, hemopericardium, purulent exudates, or effusion-associated hypothyroidism (14).

CMR. The signal intensity of the thickened pericardium on electrocardiogram-gated CMR images is variable in AP, and there is no pathognomonic intensity pattern. Signal intensity on spin echo images is inversely related to the chronicity of the pericardial inflammation. Enhancement of the thickened pericardium after the administration of contrast material may aid in its visualization and usually suggests active inflammation characteristic of AP (15) (Fig. 2). However, pericardial contrast enhancement is nonspecific

and must be interpreted within the clinical context. On CMR, transudative effusions show a low signal intensity on T_1-weighted spin echo images and a high intensity on gradient echo images such as balanced steady-state free precession (bSSFP) (15). Conversely, exudative effusions have a high protein and cell content and therefore relatively higher T_1-weighted signal intensity on spin echo images (16). Cine images with bSSFP are able to demonstrate cardiac motion within the pericardial space and delineate the bright appearance of pericardial fluid (17). This sequence allows the differentiation of structures with a high T_2/T_1 ratio, such as fluid, from ones with low ratios (myocardium), and enables a better delineation of the pericardium and the surrounding structures without the need for contrast administration.

Figure 2. Delayed Enhancement of the Pericardium

Double-inversion recovery delayed-enhancement CMR images after injection of gadolinium demonstrating circumferential enhancement of the pericardium **(arrows)** consistent with pericardial inflammation. Abbreviations as in Figure 1.

Pericardial Tamponade (PT)

PT occurs when fluid accumulation in the intra-pericardial space is sufficient to raise the pressure surrounding the heart to the point where cardiac filling is compromised.

Echocardiography. TTE should be the first modality to determine the hemodynamic significance of a pericardial effusion. The size of the effusion does not indicate its significance. On the contrary, in assessing the hemodynamic effects of an effusion, other parameters of cardiac filling must be corre-lated with the clinical context.

Persistence of right atrial (RA) inversion in ventricular systole is usually an early sign of PT, followed by diastolic compression of the right ventricular (RV) outflow tract (18–20). Right-sided chamber collapse may be delayed in the setting of pulmonary hypertension until the intrapericardial pressure is extremely high. In such cases, left atrial (LA) collapse may precede RA or RV inversion. In

most cases, due to its thicker walls and relatively lower compliance, the left ventricle (LV) is rarely seen to invert or collapse in PT. In some cases, in the setting of large pericardial effusions, the heart will be seen swinging within the pericardial fluid on a beat-to-beat basis, a finding that correlates with electrical alternans (Fig. 3B, Online Video 1).

Respiration also affects intracardiac pressures, particularly those on the right side of the heart. The normal respirophasic flow patterns are more pro-nounced in PT and can be documented by exagger-ated respiratory Doppler echocardiographic varia-tions in mitral and tricuspid inflow as well as pulmonary and systemic outflow (Fig. 3C). The percent respiratory variations in mitral inflow of >35% and tricuspid inflow of >80% correlated best with tamponade physiology in comparison studies of echocardiographic and hemodynamic measures (21–23). Respiratory variation in tricuspid and pul-monary flow is more dramatic than mitral and
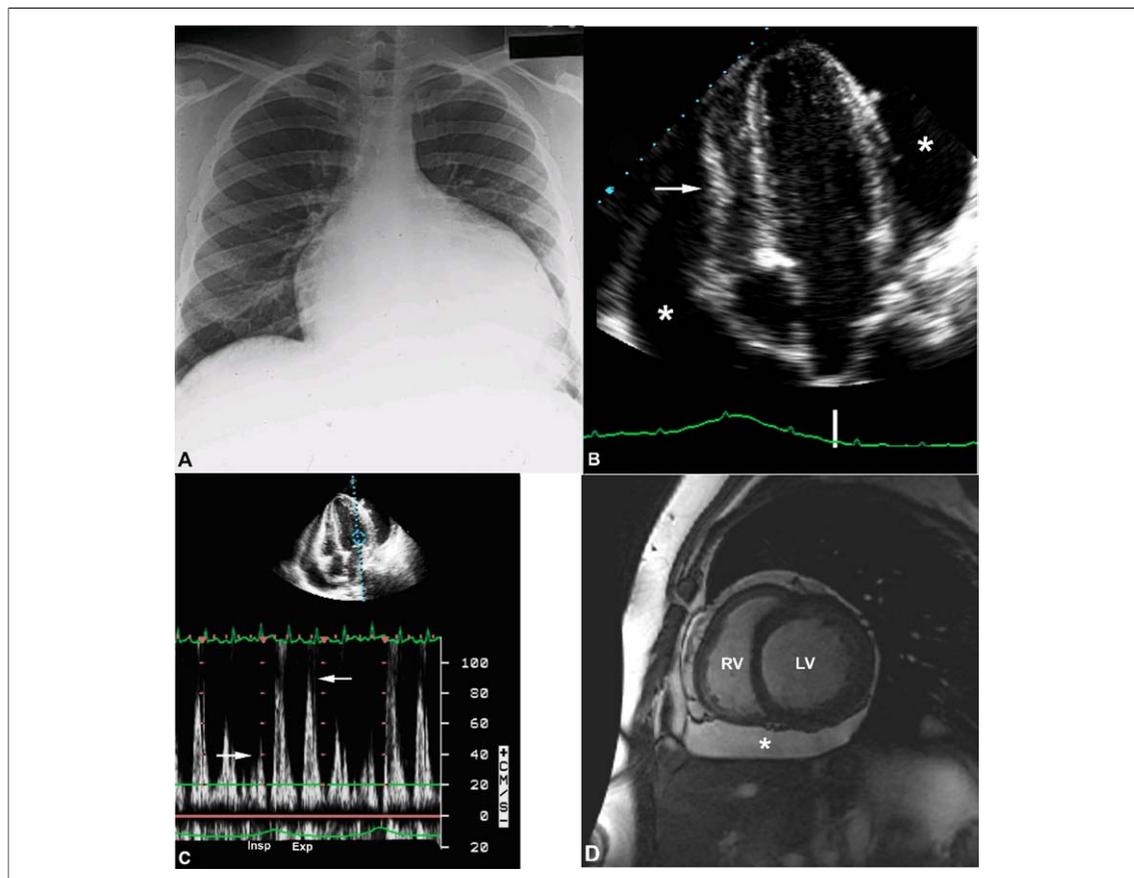

Figure 3. Imaging Findings in Pericardial Tamponade

(A) Chest radiography demonstrating the characteristic water-bottle appearance of the cardiac silhouette. **(B)** Large circumferential peri-cardial effusion with diastolic RV inversion and **(C)** reduced mitral inflow on inspiration (**arrows**). **(D)** CMR using bSSFP in a short-axis view demonstrating a circumferential pericardial effusion (*). See Online Video 1. Abbreviations as in Figure 1.

Table 1. Imaging Findings in Pericardial Tamponade

TTE
   Pericardial effusion
   RV collapse in diastole; right or left atrial collapse in systole
   Respiratory variation in mitral (>25%) and tricuspid (>40%) inflow
   Ventricular interdependence
   Plethora of IVC
   Prominence of diastolic reversals in hepatic veins by pulsed Doppler
CCT/CMR
   Presence of pericardial effusion, even if loculated or localized
   Cine CCT or CMR
     Ventricular interdependence
     Chamber collapse

CCT = cardiac computed tomography; CMR = cardiac magnetic resonance; IVC = inferior vena cava; RV = right ventricle; TTE = transthoracic echocardiography.

aortic flow, but there is progressive impairment in all intracardiac flows as the degree of tamponade worsens. Plethora of the inferior vena cava (IVC), defined as a lack of respirophasic change in IVC caliber, is a useful indicator of elevated RA pressure and is usually present in PT.

These echocardiographic findings identify changes in cardiac structure and function and the associated decrease in cardiac filling and output that often occur well before the onset of pulsus paradoxus, and thus can be an important indicator of hemodynamic compromise before it becomes clinically apparent.

CCT and CMR. Both CCT and CMR imaging are useful adjuncts to TTE in the characterization of a pericardial effusion and tamponade (Fig. 3D). They both play an important role in situations in which the hemodynamics are atypical and the presence and severity of tamponade are less certain. Both CCT and CMR provide more detailed quantification and localization of the effusion than TTE, and they are especially useful to guide pericardiocentesis, since loculated or regional effusions or regions of calcified pericardium can be identified. When hemopericardium complicates aortic dissection, CCT and CMR can readily identify the 2 diagnoses, thereby preventing inappropriate and potentially catastrophic pericardiocentesis. Real-time cine CCT and CMR imaging can also provide information similar to TTE with respect to interventricular septal (IVS) motion and chamber collapse. Modalities such as CMR, which require relatively prolonged imaging times, may not be appropriate for clinically unstable patients with suspected PT. Table 1 summarizes the imaging findings in PT.

Constrictive Pericarditis

CP represents the end stage of an inflammatory process involving the pericardium that usually takes years to develop, although it may begin several weeks after a given insult. This process results in thickening, dense fibrosis, calcification, and adhesions of the parietal and visceral pericardium.

Echocardiography. The echocardiographic diagnosis of CP, originally based on M-mode findings, now relies on 2-dimensional and Doppler hemodynamic changes in response to the respiratory cycle.

Although TTE may demonstrate pericardial thickening and calcification, its resolution may also limit it in that respect; thus transesophageal echocardiography may be more sensitive and accurate (24). Abrupt anterior or posterior motion of the IVS in early diastole is common in patients with CP (25). In classic CP, the IVS shows a brisk, early diastolic motion toward the LV during inspiration, followed by a rebound in the opposite direction during expiration (26). This motion, termed the septal bounce, reflects exaggerated interventricular dependence combined with forceful early diastolic filling (Fig. 4A and 4B; Online Video 2). Himelman et al. (27) reported that septal bounce is the most consistent echocardiographic sign for CP, with a sensitivity of 62% and specificity of 93%.

The typical diastolic transmitral Doppler findings include an increased early diastolic filling (E-wave) velocity with a rapid deceleration time (usually <160 ms) and a small or absent A-wave. The hemodynamic hallmark of CP is the exaggerated change in transvalvular flow during respiration (28) (Figs. 4A and 4C). Specifically, the mitral inflow E-wave is often relatively reduced and the isovolumic relaxation time is prolonged during inspiration, whereas with expiration, mitral inflow returns to normal and isovolumic relaxation time shortens. Typically, patients with CP demonstrate an increase in early diastolic mitral inflow of ≥25% during expiration as compared with inspiration (28,29). Sensitivities and specificities of Doppler assessment of respiratory changes have been reported to be as high as 85% to 90% (30). After complete pericardiectomy, these mitral inflow changes often return to normal, with little respiratory variation noted (29). It is noteworthy that up to 20% of patients with CP lack the typical respiratory changes in the presence of mixed constrictive-restrictive disease and/or markedly elevated LA pressure (28,31). Respirophasic changes can still be seen in patients with atrial fibrillation, although
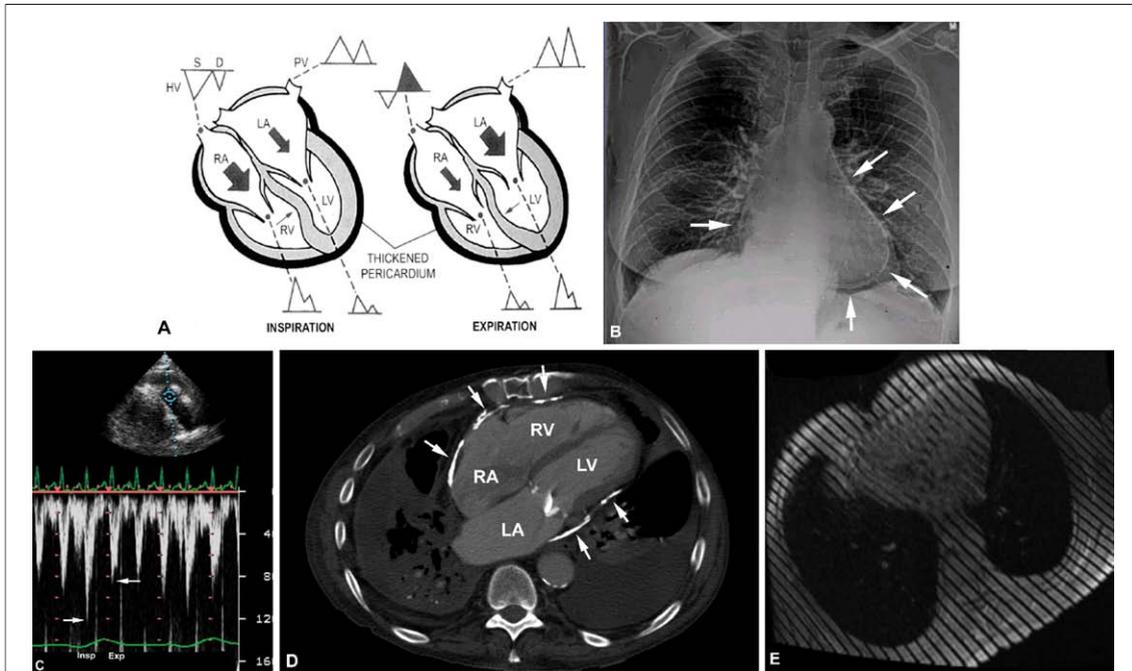
Figure 4. Multimodality Imaging in Constrictive Pericarditis

(A) Physiology of ventricular interdependence highlighting the change in transvalvular flow throughout the respiratory cycle. Reprinted with permission from Oh et al. (28). **(B)** Chest radiograph with evidence of circumferential pericardial calcification. **(C)** Pulsed-wave Doppler interrogation across the right ventricular outflow tract demonstrating significant respirophasic variation. **(D)** Cardiac computed tomography findings of pericardial calcification clustered around the atrioventricular grooves **(arrows)**. **(E)** Persistent continuity of tag lines on CMR tagging sequence throughout the cardiac cycle is diagnostic of pericardial adhesions. See Online Video 2. D = diastole; HV = hepatic veins; LA = left atrium; PV = pulmonary veins; S = systole; other abbreviations as in Figure 1.

Doppler recordings need to be longer for optimal assessment.

Inferior vena cava dilation and pulsed-wave Doppler of hepatic venous flow can be used as estimates of RA pressure. In CP, marked diastolic flow reversal that increases in expiration is evident in the hepatic veins (32). Doppler evaluation of the pulmonary veins also shows marked respiratory change in pulmonary venous flow. Both systolic and diastolic wave velocities are increased in expiration (29).

Other important findings on TTE in CP include early diastolic, rapid flattening of the posterior wall of the LV (33); normal or exaggerated longitudinal deformation of the LV base and longitudinal early diastolic tissue Doppler velocities (typically >8 cm/s) (34); reduced circumferential strain in combination with preserved longitudinal early diastolic velocities (35); as well as significantly reduced LV twist and torsion (35).

CCT. A CCT scan is able to detect even minute amounts of calcification, a finding highly suggestive of CP (36). Irregular calcification may be found anywhere over the surface of the heart, but is primarily found in regions where pericardial fat is abundant, i.e., the atrioventricular groove (Fig. 4D). Other findings of CP on CCT include a pericardial thickness of >4 mm (diffuse or localized), narrowing and tubular deformation of the RV, normal or small ventricular size, and straightening of the IVS. Additional secondary findings include signs of impaired diastolic filling of the RV: dilatation of the IVC, hepatic veins, and RA, as well as hepatosplenomegaly, ascites, and pleural effusions. If there is clinical evidence of impaired filling, pericardial thickening is virtually diagnostic of CP. The absence of thickening, however, does not rule out the presence of constriction (37). In patients being considered for pericardiectomy, detailed descriptions of the location and severity of thickening and calcification will aid the surgeon with respect to both risk stratification and planning of the procedure.

CMR. Because the pericardium is outlined by fat and lung tissue, an accurate measurement of pericardial thickness using CMR is clinically feasible with a reported accuracy of 93% when the pericardium is >4 mm thick (38). Changes similar to

Table 2. Imaging Findings in Constrictive Pericarditis

	Sensitivity	Specificity
Chest radiography		
Pericardial calcification		
Pulmonary vascular congestion		
TTE		
>35% respiratory variation of peak early diastolic MV inflow velocity (28)	88	67
Augmented hepatic vein diastolic flow reversals after the onset of expiration (28)	88	67
IVS bounce (2D TTE) (27)	62	93
Pericardial thickening (≥3 mm)		
2D TTE (28)	36	NA
TEE (24)	95	86
Longitudinal E′ tissue velocity (≥8 cm/s) (34)	89	100
CCT/CMR		
Pericardial calcification, CCT		
Pericardial thickening ≥4 mm (38)	88	100
Abnormal diastolic septal motion (42)	81	100
Narrowing, tubular deformation of RV		
Systemic venous hypertension		
Pericardial adhesions		

2D = two-dimensional; IVS = interventricular septum; MV = mitral valve; TEE = transesophageal echocardiography; other abbreviations as in Table 1.

those seen on CCT can also be seen on CMR. The thickened pericardium appears as a dark, low-intensity signal stripe sometimes demonstrating focal or diffuse, irregular, fibrocalcific changes. Calcification may not be visualized very well on CMR, and therefore CCT may be more useful for this purpose (39). Spin echo sequences are useful to detect thickened pericardium (38), whereas focal pericardial thickening and pericardial effusions are better visualized using cine gradient echo images
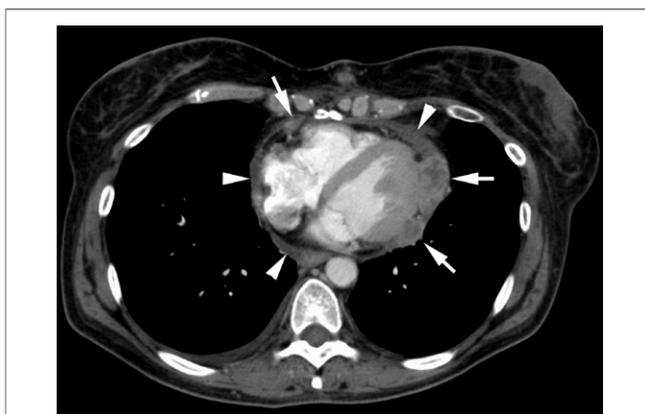

Figure 5. Computed Tomography of the Chest in a Patient With Metastatic Disease

Axial view demonstrating circumferential pericardial thickening (**arrowheads**) and deposition of pericardial metastases (**arrows**).

sensitive to pericardial fluid (40). Additional CMR findings of CP are similar to those previously discussed for CCT and include an elongated and narrowed RV, RA enlargement, and abnormal septal motion (41). Abnormal diastolic septal motion on CMR yields a sensitivity of 81% and a specificity of 100% for the diagnosis of CP (42). CMR myocardial tagging uses a grid-like pattern of saturated areas over a certain image slice and allows for the study of the deformation of the grid over time. As such, a tagging sequence can be used to evaluate adherence and immobility of the pericardial-myocardial interface (Fig. 4E). The imaging findings in CP are summarized in Table 2.

Effusive Constrictive Pericarditis

A number of patients with pericardial disease present with a clinical syndrome that combines the acute elements of pericardial effusion/PT and the chronic features of CP. These patients are sometimes identified as having effusive-CP when hemodynamics do not normalize after adequate drainage of the effusion (43). Pericardiocentesis may relieve the symptoms of PT but may then precipitate symptoms of CP (44).

Noninvasive imaging of this clinical entity combines elements of pericardial effusion, a thickened pericardium, and hemodynamic evidence of constrictive physiology and can be readily demonstrated by TTE or CMR. This entity can be considered as an intermediate transition from AP/PT to CP (44).

Pericardial Masses

Tumors. Primary pericardial tumors are rare, with mesothelioma being the most frequent. Sarcoma, lipoma, hemangioma, and teratoma can also occur in the pericardium. Secondary tumors of the pericardium are far more common. These involve local invasion of lung, mediastinal malignancies, and distal metastases. Lymphomas, melanomas, and lung and breast carcinomas are the most common metastatic tumors that involve the pericardium (45). Occasionally, pericardial masses are incidentally noted on routine TTE; however, their characterization, especially the identification/differentiation of infiltration of the adjacent structures, i.e., the myocardium, is often difficult. Consequently, CCT or CMR are often the imaging modalities of choice when further evaluating pericardial masses.

CCT and CMR. Most neoplasms are best evaluated using CMR or CCT. By CMR, these show me-

dium signal intensity on T_1-weighted spin echo images and high signal intensity on T_2-weighted spin echo images (15,46). Melanoma is an exception, with a characteristic high intensity on T_1-weighted images. A pericardial hemorrhagic effusion, caused by a malignant primary or secondary tumor of the heart or pericardium, can be easily recognized by CMR or CCT. Owing to their vascularity, pericardial metastases usually enhance after contrast administration (Fig. 5) (15).

Cysts and diverticula. Pericardial cysts are rare, benign congenital malformations. They are usually fluid filled, and may be identified as an incidental finding on chest radiography or TTE. Seventy percent of them are located at the right costophrenic angle, 22% in the left, and the rest are in the posterior or anterior superior mediastinum (47). They vary in size with a reported range of 2 to 28 cm^2. Although most cysts are benign, their rupture is a rare cause of PT.

Pericardial diverticula are rare and consist of an out-pouching of the pericardial sac. Distinction from a cyst, when possible, is based on the presence of a communication with the pericardial space, identified by changes in size related to body position (48).

Echocardiography. A cyst appears as a loculated, echo-free space adjacent to the cardiac border, most commonly near the RA, and frequently distorts the normal shape of the atrium (Fig. 6A). Contrast echocardiography may be used to exclude an anomalous systemic vein that may present in that location. Color-flow and pulsed-Doppler interrogation at low-velocity setting can be used to ensure that there is no phasic flow within that structure (33).

CCT and CMR. Contrast CCT scan has been the modality of choice to diagnose pericardial cysts as it provides superior imaging compared with other modalities (49). On CCT, pericardial cysts are thin-walled, sharply defined, oval homogeneous masses. Their attenuation is slightly higher than water at 30 to 40 HU, and they fail to enhance with intravenous contrast (50). On CMR, the characteristic appearance is that of intermediate to low intensity on T_1-weighted sequences and high signal intensity on T_2-weighted sequences. These lesions do not typically enhance with contrast ad-
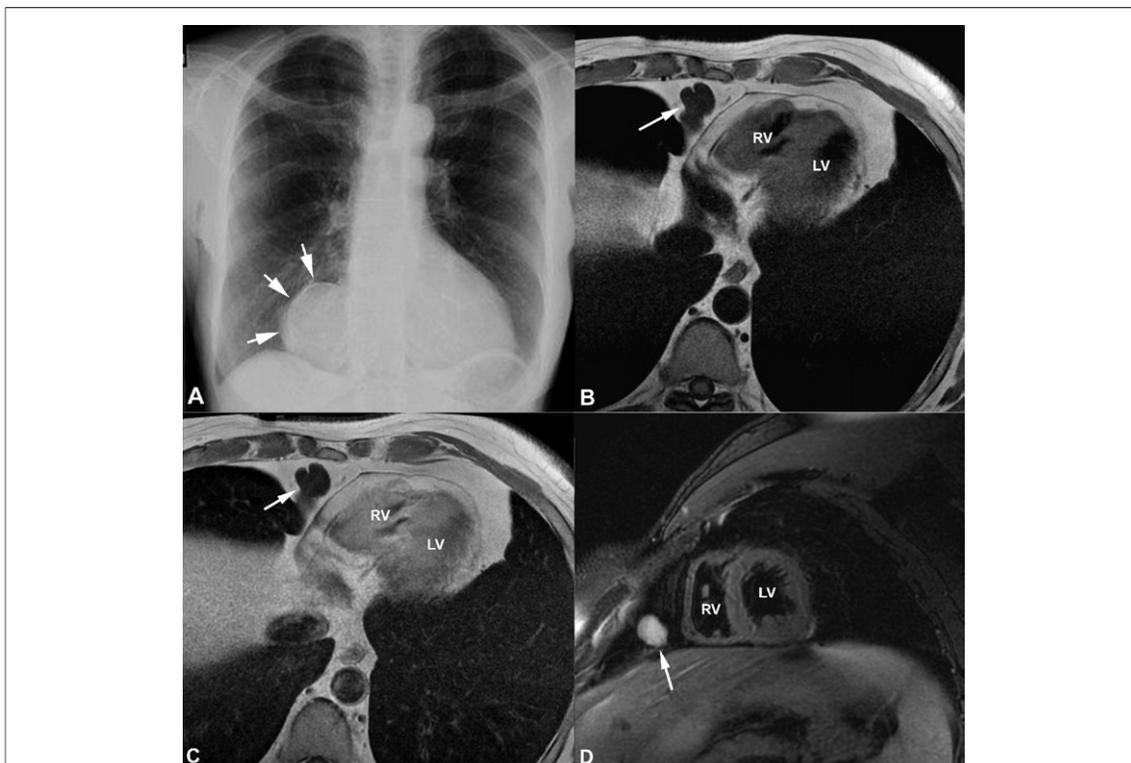
Figure 6. Multimodality Imaging of a Pericardial Cyst

(A) Chest radiograph showing a large pericardial cyst at the right costophrenic angle. In a different patient, CMR T_1-weighted spin echo imaging before (B) and after (C) gadolinium injection showing a circular, septated, hypointense, nonenhancing structure within the paracardiac fat pad at the right costophrenic angle. The hyperintense appearance on subsequent T_2-weighted spin echo imaging (D) is consistent with the diagnosis of a pericardial cyst. Abbreviations as in Figure 1.

ministration (Figs. 6B and 6C) (51). Both echocardiography (assuming adequate imaging windows are present) and contrast CCT can usually be used for follow-up, although the frequency of follow-up has not been established. As their course is usually benign, one must keep in mind the added radiation dose when following up these lesions by CCT.

Congenital Absence of Pericardium

Congenital absence of the pericardium is a rare anomaly. In surgical and pathologic series, the reported prevalence is approximately 0.002% to 0.004% (52). The defects, classified as partial or complete, are most commonly located on the left side of the heart but can be located anywhere in the pericardium. Complete defects are of little clinical importance. A subgroup of partial defects, the

Figure 7. Multimodality Imaging of Congenital Absence of the Pericardium

Chest radiograph **(A)** and chest cardiac computed tomography scan **(B)** demonstrating superior and lateral displacement of the apex without identifiable pericardium over the apex of the heart consistent with congenital absence of the pericardium. Abbreviations as in Figure 1.

foramen-type defects, can be fatal when they allow herniation of a part of the heart.

Echocardiography. With a defect in the pericardium, cardiac motion, especially the posterior wall of the LV, is exaggerated. The RV cavity may falsely appear enlarged due to the shifting of the entire cardiac structure to the left. Other TTE signs include the displacement of the apical imaging window into the axilla and the appearance of compressed atria.

CCT and CMR. Although the pericardium is usually sufficiently thick to be identified on CCT and CMR, visualization at the most common site of pericardial defects, the lateral, posterior, and inferior left ventricular wall, can be poor because of a paucity of fat (53). Several indirect morphologic signs have been accepted as diagnostic of pericardial defects. Interposition of lung tissue between the aorta and pulmonary artery or between the diaphragm and the base of the heart is the most specific sign and occurs in all patients with complete left pericardial defects or partial defects overlying these anatomic structures (54). Leftward cardiac displacement usually accompanies complete left pericardial absence, and excessive levorotation has been proposed as pathognomonic of this type of defect (55) (Fig. 7). Nevertheless, cardiac displacement also can occur in left partial pericardial defects (54) or can be absent in young children with complete pericardial defects (55). Patients with pericardial defects also may have one or more associated congenital abnormalities, including atrial septal defect, patent ductus arteriosus, mitral valve stenosis, or tetralogy of Fallot (56), which are also detectable by CCT or CMR.
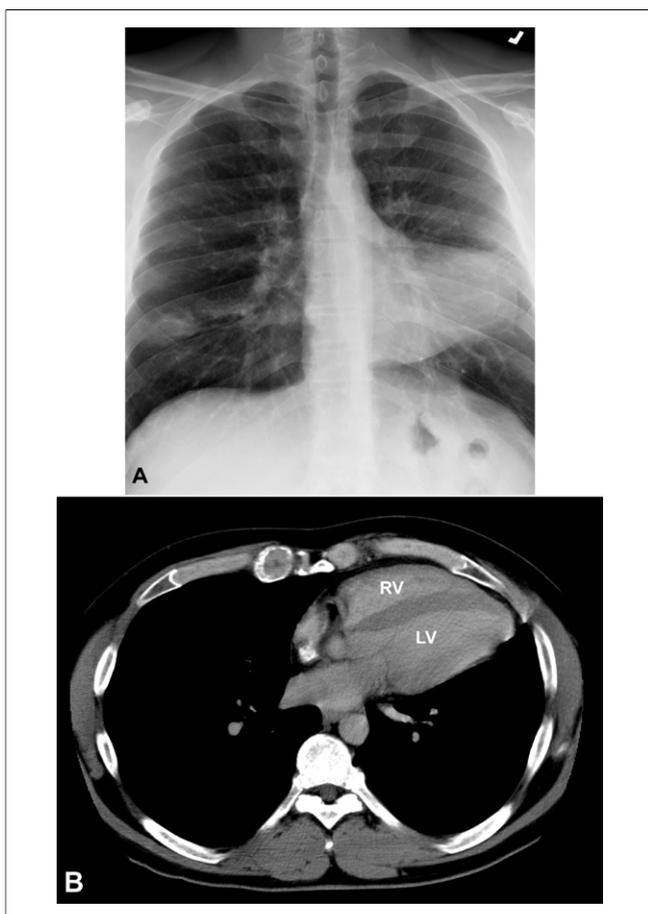
Conclusions

The pericardium can be affected by a wide variety of primary processes and systemic diseases. Echocardiography remains the initial diagnostic imaging modality of choice due to its availability and affordability. It performs particularly well in the diagnosis of pericardial effusions, tamponade, and CP. On the other hand, both CCT and CMR are becoming more widely available and provide novel and complementary information with respect to the morphologic and functional features of the diseased pericardium. Although they should not replace echocardiography as first-line imaging, they should be used when findings on TTE are difficult to interpret or conflict with clinical findings.

REFERENCES

1. LeWinter MM, Kabbani S. Pericardial diseases. In: Zipes DP, Libby P, Bonow RO, et al., editors. Heart Disease: A Textbook of Cardiovascular Medicine. 7th edition. Philadelphia, PA: Elsevier, 2005:1757–80.

2. Spodick DH. Macrophysiology, microphysiology, and anatomy of the pericardium: a synopsis. Am Heart J 1992;124:1046–51.

3. Bull RK, Edwards PD, Dixon AK. CT dimensions of the normal pericardium. Br J Radiol 1998;71:923–5.

4. Frank H, Globits S. Magnetic resonance imaging evaluation of myocardial and pericardial disease. J Magn Reson Imaging 1999;10:617–26.

5. Mahabadi AA, Massaro JM, Rosito GA, et al. Association of pericardial fat, intrathoracic fat, and visceral abdominal fat with cardiovascular disease burden: the Framingham Heart Study. Eur Heart J 2009;30:850–6.

6. Truong QA, Siegel E, Cannon CP. Cardiac CT angiography—radiation dose—how effective are we in reducing radiation dose from cardiac CT angiography? Rev Cardiovasc Med 2009;10:236–9.

7. Ronan PK, Jonathan DD, Ricardo CC. Noncardiac findings on cardiac CT part I: pros and cons. 2009;3:293–9.

8. Maisch B, Seferovic PM, Ristic AD, et al. Guidelines on the diagnosis and management of pericardial diseases executive summary; The Task Force on the Diagnosis and Management of Pericardial Diseases of the European Society of Cardiology. Eur Heart J 2004;25:587–610.

9. Lange RA, Hillis LD. Clinical practice. Acute pericarditis. N Engl J Med 2004;351:2195–202.

10. Troughton RW, Asher CR, Klein AL. Pericarditis. Lancet 2004;363:717–27.

11. Cheitlin MD, Armstrong WF, Aurigemma GP, et al. ACC/AHA/ASE 2003 guideline update for the clinical application of echocardiography: summary article: a report of the American College of Cardiology/American Heart Association Task Force on Practice Guidelines (ACC/AHA/ASE Committee to Update the 1997 Guidelines for the Clinical Application of Echocardiography). Circulation 2003;108:1146–62.

12. Chandraratna PA. Echocardiography and Doppler ultrasound in the evaluation of pericardial disease. Circulation 1991;84:I303–10.

13. Ordovas KG, Higgins CB. Pericardial diseases. In: McAllisster L, Barrett K, editors. MRI and CT of the Cardiovascular System. 1st edition. Philadelphia, PA: Lippincott, 2006:137–53.

14. Tomoda H, Hoshiai M, Furuya H, et al. Evaluation of pericardial effusion with computed tomography. Am Heart J 1980;99:701–6.

15. Wang ZJ, Reddy GP, Gotway MB, et al. CT and MR imaging of pericardial disease. Radiographics 2003;23 Spec No:S167–80.

16. Hancock EW. Neoplastic pericardial disease. Cardiol Clin 1990;8:673–82.

17. Kovanlikaya A, Burke LP, Nelson MD, et al. Characterizing chronic pericarditis using steady-state free-precession cine MR imaging. AJR Am J Roentgenol 2002;179:475–6.

18. Armstrong WF, Schilt BF, Helper DJ, et al. Diastolic collapse of the right ventricle with cardiac tamponade: an echocardiographic study. Circulation 1982;65:1491–6.

19. Gillam LD, Guyer DE, Gibson TC, et al. Hydrodynamic compression of the right atrium: a new echocardiographic sign of cardiac tamponade. Circulation 1983;68:294–301.

20. Singh S, Wann LS, Schuchard GH, et al. Right ventricular and right atrial collapse in patients with cardiac tamponade—a combined echocardiographic and hemodynamic study. Circulation 1984;70:966–71.

21. Gonzalez MS, Basnight MA, Appleton CP. Experimental cardiac tamponade: a hemodynamic and Doppler echocardiographic reexamination of the relation of right and left heart ejection dynamics to the phase of respiration. J Am Coll Cardiol 1991;18:243–52.

22. Picard MH, Sanfilippo AJ, Newell JB, et al. Quantitative relation between increased intrapericardial pressure and Doppler flow velocities during experimental cardiac tamponade. J Am Coll Cardiol 1991;18:234–42.

23. Schutzman JJ, Obarski TP, Pearce GL, et al. Comparison of Doppler and two-dimensional echocardiography for assessment of pericardial effusion. Am J Cardiol 1992;70:1353–7.

24. Ling LH, Oh JK, Tei C, et al. Pericardial thickness measured with transesophageal echocardiography: feasibility and potential clinical usefulness. J Am Coll Cardiol 1997;29:1317–23.

25. Voelkel AG, Pietro DA, Folland ED, et al. Echocardiographic features of constrictive pericarditis. Circulation 1978;58:871–5.

26. Candell-Riera J, Garcia del Castillo H, Permanyer-Miralda G, et al. Echocardiographic features of the interventricular septum in chronic constrictive pericarditis. Circulation 1978;57:1154–8.

27. Himelman RB, Lee E, Schiller NB. Septal bounce, vena cava plethora, and pericardial adhesion: informative two-dimensional echocardiographic signs in the diagnosis of pericardial constriction. J Am Soc Echocardiogr 1988;1:333–40.

28. Oh JK, Hatle LK, Seward JB, et al. Diagnostic role of Doppler echocardiography in constrictive pericarditis. J Am Coll Cardiol 1994;23:154–62.

29. Hatle LK, Appleton CP, Popp RL. Differentiation of constrictive pericarditis and restrictive cardiomyopathy by Doppler echocardiography. Circulation 1989;79:357–70.

30. Hancock EW. Differential diagnosis of restrictive cardiomyopathy and constrictive pericarditis. Heart 2001;86:343–9.

31. Oh JK, Tajik AJ, Appleton CP, et al. Preload reduction to unmask the characteristic Doppler features of constrictive pericarditis. A new observation. Circulation 1997;95:796–9.

32. von Bibra H, Schober K, Jenni R, et al. Diagnosis of constrictive pericarditis by pulsed Doppler echocardiography of the hepatic vein. Am J Cardiol 1989;63:483–8.

33. Feigenbaum H. Echocardiography. 6th edition. Philadelphia, PA: Lippincott, 2005.

34. Rajagopalan N, Garcia MJ, Rodriguez L, et al. Comparison of new Doppler echocardiographic methods to differentiate constrictive pericardial heart disease and restrictive cardiomyopathy. Am J Cardiol 2001;87:86–94.

35. Sengupta PP, Krishnamoorthy VK, Abhayaratna WP, et al. Disparate patterns of left ventricular mechanics differentiate constrictive pericarditis from restrictive cardiomyopathy. J Am Coll Cardiol Img 2008;1:29–38.

36. Isner JM, Carter BL, Bankoff MS, et al. Computed tomography in the diagnosis of pericardial heart disease. Ann Intern Med 1982;97: 473–9.

37. Talreja DR, Edwards WD, Danielson GK, et al. Constrictive pericarditis in 26 patients with histologically normal pericardial thickness. Circulation 2003;108:1852–7.

38. Masui T, Finck S, Higgins CB. Constrictive pericarditis and restrictive cardiomyopathy: evaluation with MR imaging. Radiology 1992;182: 369–73.

39. Maksimovic R, Seferovic PM, Ristic AD, et al. Cardiac imaging in rheumatic diseases. Rheumatology (Oxford) 2006;45 Suppl 4:iv26–31.

40. Axel L. Assessment of pericardial disease by magnetic resonance and computed tomography. J Magn Reson Imaging 2004;19:816–26.

41. Rienmuller R, Groll R, Lipton MJ. CT and MR imaging of pericardial disease. Radiol Clin North Am 2004; 42:587–601.

42. Giorgi B, Mollet NR, Dymarkowski S, et al. Clinically suspected constrictive pericarditis: MR imaging assessment of ventricular septal motion and configuration in patients and healthy subjects. Radiology 2003;228:417–24.

43. Hancock EW. Subacute effusive-constrictive pericarditis. Circulation 1971;43:183–92.

44. Hancock EW. A clearer view of effusive-constrictive pericarditis. N Engl J Med 2004;350:435–7.

45. Klatt EC, Heitz DR. Cardiac metastases. Cancer 1990;65:1456–9.

46. Hoffmann U, Globits S, Frank H. Cardiac and paracardiac masses. Current opinion on diagnostic evaluation by magnetic resonance imaging. Eur Heart J 1998;19:553–63.

47. Borges AC, Gellert K, Dietel M, et al. Acute right-sided heart failure due to hemorrhage into a pericardial cyst. Ann Thorac Surg 1997;63:845–7.

48. Jeung MY, Gasser B, Gangi A, et al. Imaging of cystic masses of the mediastinum. Radiographics 2002;22 Spec No:S79–93.

49. Patel J, Park C, Michaels J, et al. Pericardial cyst: case reports and a literature review. Echocardiography 2004;21:269–72.

50. Demos TC, Budorick NE, Posniak HV. Benign mediastinal cysts: pointed appearance on CT. J Comput Assist Tomogr 1989;13:132–3.

51. Vinee P, Stover B, Sigmund G, et al. MR imaging of the pericardial cyst. J Magn Reson Imaging 1992;2:593–6.

52. Yamano T, Sawada T, Sakamoto K, et al. Magnetic resonance imaging differentiated partial from complete ab-

sence of the left pericardium in a case of leftward displacement of the heart. Circ J 2004;68:385–8.

53. Baim RS, MacDonald IL, Wise DJ, et al. Computed tomography of absent left pericardium. Radiology 1980;135: 127–8.

54. Gatzoulis MA, Munk M-D, Merchant N, et al. Isolated congenital absence of the pericardium: clinical presentation, diagnosis, and management. Ann Thorac Surg 2000;69: 1209–15.

55. Gassner I, Judmaier W, Fink C, et al. Diagnosis of congenital pericardial defects, including a pathognomic sign for dangerous apical ventricular herniation, on magnetic resonance imaging. Br Heart J 1995;74:60–6.

56. Spodick D. Pericardial disease. In: Braunwald E, Zipes DP, Libby P, editors. Heart Disease: A Textbook of Cardiovascular Medicine. 6th edition. Philadelphia, PA: Saunders, 2007: 1823–76.

Key Words: pericarditis ■ echocardiography ■ cardiac computed tomography ■ cardiac magnetic resonance.

⊞ APPENDIX

For supplementary videos and their legends, please see the online version of this article.